Published in final edited form as:
Mol Pharm. 2008 ; 5(6): 1122–1130.

Targeted Disruption of Peptide Transporter *Pept1* Gene in Mice Significantly Reduces Dipeptide Absorption in Intestine

Yongun Hu[†], **David E. Smith**[*,†], **Ke Ma**[†], **Dilara Jappar**[†], **Winston Thomas**[‡], and **Kathleen M. Hillgren**[§]
Department of Pharmaceutical Sciences, University of Michigan, Ann Arbor, Michigan, Deltagen, San Mateo, CA, and Lilly Research Laboratories, Eli Lilly and Company, Indianapolis, Indiana

Abstract

PEPT1 is a high-capacity, low-affinity peptide transporter that mediates the uptake of di- and tripeptides in the intestine and kidney. PEPT1 also has significance in its ability to transport therapeutic agents and because of its potential as a target for anti-inflammatory therapies. To further understand the relevance of specific peptide transporters in intestinal physiology, pharmacology and pathophysiology, we have generated *Pept1* null mice by targeted gene disruption. The *Pept1* gene was disrupted by insertion of a *lacZ* reporter gene under the control of the endogenous *Pept1* promoter. Phenotypic profiling of wild-type and *Pept1* null mice was then performed, along with *in vitro* intestinal uptake, *in situ* intestinal perfusion and *in vivo* pharmacokinetic studies of glycylsarcosine (GlySar). *Pept1* null mice lacked expression of PEPT1 protein in the intestine and kidney, tissues in which this peptide transporter is normally expressed. *Pept1*-deficient mice were found to be viable, fertile, grew to normal size and weight, and were without any obvious abnormalities. Nevertheless, *Pept1* deletion dramatically reduced the intestinal uptake and effective permeability of the model dipeptide GlySar (i.e., by at least 80%), and its oral absorption following gastric gavage (i.e., by about 50%). In contrast, the plasma profiles of GlySar were almost superimposable between wild-type and *Pept1* null animals after intravenous dosing. These novel findings provide strong evidence that PEPT1 has a major role in the *in vivo* oral absorption of dipeptides.

Keywords

targeted disruption; knockout mice; Pept1; dipeptides; intestinal absorption

Introduction

In mammals, the proton-coupled oligopeptide transporter (POT) family consists of four members [i.e., PEPT1 (SLC15A1), PEPT2 (SLC15A2), PHT1 (SLC15A4), PHT2 (SLC15A3)] and is responsible for the symport of small peptides/mimetics across biological membranes via an inwardly-directed proton gradient and negative membrane potential.[1-4] The POT proteins vary in size from 572-729 amino acids and are predicted to contain 12 transmembrane domains, with the N- and C-termini facing the cytosol. The encoded proteins have a number of potential protein kinase recognition domains (i.e., 0-3 for PKA, 1-11 for

*To whom correspondence should be addressed. Mailing address: University of Michigan, Upjohn Center for Clinical Pharmacology, 4742 Medical Sciences II, 1150 W. Medical Center Drive, Ann Arbor, Michigan 48109-5633. Phone: 734-647-1431. Fax: 734-763-3438. E-mail: smithb@umich.edu..
[†]Department of Pharmaceutical Sciences, University of Michigan.
[‡]Deltagen
[§]Eli Lilly and Company

PKC) and glycosylation sites (i.e., 2-7); however, their relevance has not been proven experimentally. Whereas PEPT1 and PEPT2 have high homology between species (about 80% in rat, rabbit, human and mouse), the homology between these two transporters for a given species is low (about 50%). Rat PHT1 and PHT2 have an amino acid identity of about 50%, but they show little homology to either PEPT1 or PEPT2 (less than 20%).

PEPT1, a high-capacity low-affinity transporter, has nutritional importance because of its role in the intestinal absorption of small peptides from the diet and because of its role in the reabsorption of peptide-bound amino nitrogen from glomerular filtrate in kidney. PEPT1 also has significance in its ability to transport therapeutic agents (e.g., β-lactam antibiotics, angiotensin-converting enzyme inhibitors, antiviral nucleoside prodrugs) and potentially toxic peptidomimetics (e.g., 5-aminolevulinic acid). Immunolocalization studies demonstrated that PEPT1 was expressed in the apical membrane of enterocytes in the small intestine (i.e., duodenum, jejunum and ileum) with little or no expression in normal colon.[5,6] PEPT2, a low-capacity high-affinity transporter, has been reported in glial cells and tissue-resident macrophages of the enteric nervous system.[7] However, it is unlikely that PEPT2-mediated absorption is involved in these deep, neuromuscular layers of the gastrointestinal tract. Likewise, transcripts of the peptide-histidine transporters PHT1 and PHT2 have been reported in intestinal tissue segments,[8] but their role in peptide/mimetic absorption has not been demonstrated.

More recently, it has been shown that in chronic states of intestinal inflammation, such as in Crohn's disease and ulcerative colitis, PEPT1 expression is induced in colonic epithelia.[9] Under such conditions, bacterially-derived chemotactic peptides (e.g., fMet-Leu-Phe and Ac-muramyl-Ala-Glu) can gain access to the intracellular compartment of epithelial cells and/or immune cells within the lamina propria. This unique relationship suggests an involvement of PEPT1 in inflammatory bowel disease and the innate immune response, as well as a novel target for anti-inflammatory therapies.[10]

While cellular, molecular and physiological studies have made major contributions toward a mechanistic understanding of PEPT1 structure, function and localization, the experimental approaches are often limited by an *in vitro* design and lack of blood supply, overlapping substrate specificities and contribution of multiple transport systems, some of which are unknown at the time of study. As a result, it is difficult, if not impossible, to define the function of a single specific gene product and its significance in relation to other possible proteins that are present in the tissue or organ of interest.

In the present study, we describe for the first time the development, validation, and phenotypic analysis of transgenic mice lacking the *Pept1* gene. Our findings demonstrate that PEPT1 is responsible for at least 80% of glycylsarcosine (GlySar) uptake during studies using *in vitro* intestinal rings and *in situ* single-pass intestinal perfusions. Moreover, the results are corroborated by *in vivo* studies in which *Pept1* deletion substantially reduces the oral absorption and systemic exposure of this dipeptide.

Materials and Methods

Animals

Animal studies were conducted in accordance with the Guide for the Care and Use of Laboratory Animals as adopted and promulgated by the U.S. National Institutes of Health. Gender- and weight-matched wild-type (*Pept1*$^{+/+}$) and null (*Pept1*$^{-/-}$) mice (>99% C57BL/6 genetic background), 8 to 10 weeks of age, were used for all phenotypic analyses unless otherwise noted. The mice were kept in a temperature-controlled environment with a 12-hr

light and 12-hr dark cycle, and received a standard diet and water *ad libitum* (Unit for Laboratory Animal Medicine, University of Michigan, Ann Arbor, MI).

Construction of Targeting Vector and Generation of Pept1 Null Mice

Pept1 null mice were obtained from Deltagen, Inc (San Mateo, CA) and were developed using a conventional transgenic and breeding strategy, as described previously.[11] Briefly, a genomic fragment of about 5.6 kb, including protein coding regions of the *Pept1* gene (slc15a1), was isolated from a mouse genomic library and subcloned into the Bam HI site of the pBluescript II SK(-) vector. Bases from +77 to +101 were deleted from a segment of the protein coding region and replaced with an IRES-lacZ reporter and neomycin (G418) resistance cassette of about 6.9 kb. This mutation was designed to produce a loss-of-function mutation by deletion of amino acids 16 to 24. The IRES-lacZ-neo cassette was flanked by 2.8 kb of mouse genomic DNA at the 5' arm and by 2.8 kb of genomic DNA at the 3' arm. The targeting vector was then linearized and electroporated into ES cells derived from the 129P2/OlaHsd mouse substrain. The ES cells were selected for G418 resistance, and colonies that had integrated the IRES lacZ-neo DNA were identified by PCR amplification using three neo-specific primers paired with primers located outside the targeting homology arms of vector (i.e., AAGGCTCTTCTTGGCTGACTGTAGC for 5' and TTAAGCATGGAATGGACATGGTCTC for 3', respectively). Male chimeric mice, generated by injection of the targeted ES cells into C57BL/6 blastocysts, were bred with C57BL/6 mice to produce F1 heterozygous (*Pept1*$^{+/-}$) mice. F2 homozygous mutant mice were then produced by intercrossing F1 heterozygous males and females. PCR was used to confirm germline transmission and the subsequent production of congenic *Pept1* null mice on a C57BL/6 background ($\geq$ 99%).

Taqman Real-Time PCR Analyses

Quantitation of PHT1 and PHT2 transcripts was performed on the small intestine, colon and kidney from wild-type and *Pept1* null mice using the 7300 Real-Time PCR System (Applied Biosystems, Foster City, CA). Total RNA was isolated according to the manufacturer's protocol using the RNeasy Plus Mini Kit (Qiagen, Valencia, CA), and then reverse-transcribed. The PHT1 and PHT2 primers and probes were designed with Primer Express 3.0 software (Applied Biosystems, Foster City, CA), and the primers, probes and standard DNA were synthesized by Integrated DNA Technologies (Coralville, IA). The forward and reverse primers and probe for PHT1 were: GGCCATTGGGTGGATGAG, GCAGGTGGCAGCTGTTGA and 5'-/56-FAM/-CTGGCCGCCATCCAGGGAGC-/36-TAMSp/-3', respectively; the forward and reverse primers and probe for PHT2 were: CCTGTGATGGTGACCCTTGTG, GGAGGACATAGGTGGACTGCAT and 5'-/56-FAM/-CTGCTGTCCCTGCCGGAAGTCCT-/36-TAMSp/-3', respectively. The forward and reverse primers and probe for GAPDH were: GAGACAGCCGCATCTTCTTGT, CACACCGACCTTCACCATTTT and 5'-/Joe/-CAGTGCCAGCCTCGTCCCGTAGA-/36-TAMSp/-3', respectively. The thermal profile was 1 cycle at 50°C for 2 min, 1 cycle at 95°C for 10 min, 40 cycles at 95°C for 15 sec and 60°C for 1 min. The absolute amount of PHT1 and PHT2 transcripts was calculated automatically based on the standard curve, and then normalized for GAPDH.

Immunoblot Analyses

Brush border membrane vesicles were prepared from the intestine and kidneys from wild-type and *Pept1* null mice, as described previously.[12,13] The membrane proteins were resolved on 7.5% SDS-PAGE, transferred to a PVDF membrane, and blotted with specific polyclonal rat PEPT1 antisera[14,15] (1:500 dilution) or mouse PEPT2 antisera (raised against the COOH-terminal region, KQIPHIQGNMINLETKNTRL, amino acids 721-740; Lampire Biological

Laboratories, Pipersville, PA) (1:5000 dilution). The filters were washed three times with TBS-T and then incubated with goat anti-rabbit IgG conjugated to horseradish peroxidase (Bio-Rad, Hercules, CA) (1:3000 dilution). For β-actin, the membrane was blotted with a mouse monoclonal antibody (Santa Cruz Biotechnology, Santa Cruz, CA) (1:1000 dilution) followed by the secondary antibody, goat anti-mouse IgG conjugated to horseradish peroxidase (Santa Cruz Biotechnology, Santa Cruz, CA) (1:3000 dilution). The membranes were then washed five times in TBS-T, and the bound antibody was detected with Immobilon Western Chemiluminescent Substrate (Millipore, Billerica, MA).

In Vitro Intestinal Uptake Studies

Following an overnight fast (>12 hr), gender-matched *Pept1*$^{+/+}$ and *Pept1*$^{-/-}$ mice were anesthetized with sodium pentobarbital (40-60 mg/kg ip). Everted ring experiments were then performed according to methods described previously.[16] In brief, the abdomen was opened, the jejunum isolated (i.e., ~ 2 cm distal to the ligament of Treitz), and two 2-cm segments transferred to an ice-cold incubation medium. Following a rapid wash, the jejunal segments were everted and fixed over glass rods (3 mm outer diameter) with surgical thread. Everted segments were then equilibrated for 5 min with incubation medium, which was gassed continuously with 5%CO_2-95%O_2 in a 37°C shaking water bath. Following the equilibration period, each jejunal segment was placed in 1 ml of incubation medium containing 4 μM [^{14}C] GlySar and 4 μM [^{3}H]mannitol (an extracellular marker). After incubating for 20 sec at 37°C, each segment was rapidly washed with ice-cold incubation medium, blotted on filter paper, weighed, and solubilized in 0.33 ml of 1 M hyamine hydroxide. The contents were then transferred to a vial containing scintillation fluid for measurement of radioactivity by a dual-channel liquid scintillation counter. The incubation medium contained 129 mM NaCl, 5.1 mM KCl, 1.4 mM $CaCl_2$, 1.3 mM NaH_2PO_4, and 1.3 mM Na_2HPO_4 (pH 6.0).

In Situ Single-Pass Intestinal Perfusion Studies

Following an overnight fast (>12 hr), gender-matched *Pept1*$^{+/+}$ and *Pept1*$^{-/-}$ mice were anesthetized with sodium pentobarbital (40-60 mg/kg ip). Jejunal perfusion experiments were then performed according to methods described previously for normal and mdr1a/1b (-/-) mice.[17] In brief, surgery was performed on animals after placing them on a heating pad to maintain body temperature. The abdomen was opened and a midline longitudinal incision was made to expose the small intestine. An 8-cm segment of proximal jejunum was isolated (i.e., ~ 2 cm distal to the ligament of Treitz) followed by incisions at both the proximal and distal ends. A glass cannula (2.0 mm outer diameter) was inserted at each end of the jejunal segment and secured in place with silk sutures. Following cannulation, the isolated intestinal segment was rinsed with isotonic saline solution, and covered with saline-wetted gauze and parafilm to prevent dehydration. After the surgical procedure, the animals was transferred to a temperature-controlled chamber (31°C) to maintain body temperature during the actual perfusion experiment. The inlet cannula was connected to a 10-ml syringe placed on a perfusion pump.

The perfusate solution contained 135 mM NaCl, 5 mM KCl, and 10 mM MES (pH 6.5) plus 10 μM [^{3}H]GlySar and 0.01% [^{14}C]PEG 4000 (which served as a nonabsorble marker to correct for water flux). The solution was perfused through the intestinal segment at a rate of 0.1 ml/min, and the exiting perfusate collected every 10 min for 90 min. A 100-μl aliquot of each sample was added to a vial containing scintillation fluid for measurement of radioactivity by a dual-channel liquid scintillation counter. At the conclusion of the experiment, the intestinal segment was measured for its length.

In Vivo Pharmacokinetic Studies

Following an overnight fast (>12 hr), gender-matched *Pept1*$^{+/+}$ and *Pept1*$^{-/-}$ mice were anesthetized briefly with isoflurance prior to administration of [^{14}C]GlySar (10 nmol/g body

weight) by tail vein injection (intravenous) or gastric lavage (oral). After intravenous dosing, serial blood samples were collected at 0.25, 2, 5, 15, 30, 60, 120, 240, 360 and 480 min; after oral dosing, serial blood samples were collected at 15, 30, 45, 60, 90, 120, 180, 240, 360 and 480 min. Blood samples (15-20 μl) were obtained via tail transections and the plasma harvested. Animals were returned to their cages in between blood sampling where they had free access to water; food was provided in their cages four hours after dosing. Radioactivity in plasma was measured by a dual-channel liquid scintillation counter.

Data Analysis

Jejunal transport was determined from the steady-state loss of drug from the perfusate as it flowed through the intestine, which was achieved approximately 30-40 min after the start of perfusion. The effective permeability (*Peff*) of GlySar was calculated according to a complete mixing model:[18,19] $Peff = - Q/(2\pi RL) \cdot ln(Cout/Cin)$, where Q is the perfusate flow rate, R the intestinal radius, L the length of intestine, *Cout* the outlet drug concentration (corrected for water flux), and *Cin* the inlet drug concentration.

The pharmacokinetics of GlySar were determined by noncompartmental analysis[20] after oral and intravenous administrations using WinNonlin (version 5.0; Pharsight, Mountain View, CA).

Data are reported as mean ± SE, unless otherwise noted. Statistical differences between the wild-type and *Pept1* null mice were determined using a two sample t-test; $p \leq 0.05$ was considered significant.

Results

Targeted Disruption of the Pept1 Gene

The mouse Pept1 gene was disrupted by replacing part of the coding region of exon 3 with the IRES-LacZ-Neo cassette via homologous recombination in ES cells (Figure 1A). Correct targeting of the *Pept1* locus in ES clones was determined in both directions by PCR of the genomic DNA (Figure 1B). Heterozygous male and female mice (F1 generation) were mated to produce wild-type and *Pept1* null mouse (F2 generation). The targeted *Pept1* allele was detected in these offspring by PCR analysis of genomic DNA isolated from tail biopsies (Figure 1C).

Tissue Expression of Proton-Coupled Oligopeptide Transporters

Immunoblot analyses of intestinal and kidney membranes were performed to probe whether aberrant levels of PEPT2 protein appear in the intestine of *Pept1* null mice, or if PEPT2 protein levels in the kidney differ between genotypes. As expected, PEPT1 protein was expressed in the brush border membranes of small intestine (Figure 2A) and kidney (Figure 2B) of rat, wild-type and *Pept2* null mice. Moreover, there was a complete absence of this immunoreactive protein in the tissues of *Pept1*-deficient animals. On the other hand, PEPT2 protein was absent from the brush border membranes of small intestine (Figure 3A), and showed only a minor increase of expression in brush border membranes of kidney (Figure 3B) or whole tissue lysates (Figure 3C) of wild-type and *Pept1* null mice.

Given the lack of available antisera, real-time PCR studies (i.e., GAPDH-normalized) were performed for PHT1 and PHT2. As shown in Figure 4, there were no significant differences for PHT1 or PHT2 transcripts (Figures 4A or 4B, respectively) in the small intestine, large intestine and kidney of *Pept1*-deficient and competent mice.

Initial Phenotypic Analysis

No pathological phenotype was observed between gender-matched wild-type and *Pept1*-deficient mice. In this regard, *Pept1* null animals were found to be viable, fertile, grew to normal size, body weight and organ weight, and had no significant differences in serum clinical chemistry (Table 1). Moreover, histological examination excluded any genotype-related abnormalities of major organs (including the kidneys, and small and large intestines).

In Vitro Intestinal Uptake, In Situ Intestinal Perfusion and In Vivo Pharmacokinetic Studies

Studies in everted jejunal rings showed that GlySar uptake in *Pept1* null mice was only 22% of that observed in wild-type mice (Figure 5A). While *in vitro* intestinal uptake studies have certain advantages (in terms of simplicity, speed, and ability to study axial differences in uptake), they are limited by their lack of an intact blood supply. As a result, we also performed *in situ* jejunal perfusions of GlySar. As shown in Figure 5B, the effective permeability of GlySar in *Pept1*-deficient mice was only 5% of the value observed in wild-type animals.

Studies were performed after oral and intravenous routes of administration to probe whether or not disruption of the *Pept1* gene would affect the *in vivo* systemic kinetics and oral availability of a model dipeptide. As shown in Figure 6A, plasma concentrations of GlySar were initially about 40-50 μM after intravenous dosing and declined rapidly over time. The two curves were almost superimposable and there were no pharmacokinetic differences between wild-type and *Pept1* null animals. In particular, the clearance of GlySar differed by only 7% between the two genotypes (i.e., 0.17±0.01 and 0.16±0.01 ml/min; wild-type and null mice, respectively). In contrast, *Pept1*-deficient mice had substantially reduced peak concentrations of GlySar (i.e., 2.5±0.1 and 1.0±0.1 μM; wild-type and null mice, respectively; $p<0.001$) and areas under the curve (i.e., 641±50 and 322±10 μM·min over 8 hr; wild-type and null mice, respectively; $p<0.001$) after gastric lavage as compared to *Pept1*-competent animals (Figure 6B). These findings confirm our previous results using *in vitro* and *in situ* methods, and suggest strongly that *Pept1* deletion can significantly reduce the *in vivo* oral absorption of dipeptides.

Discussion

Proteins originating from the diet and from gastrointestinal secretions are digested by several gastric and pancreatic proteases, which are further acted upon by a cadre of peptidases in the brush border membrane of intestinal epithelium.[21] These protein digestion products then enter the enterocyte, primarily as di- and tripeptides as opposed to free amino acids. Once inside the cell, cytoplasmic peptidases act on the di-/tripeptides so that the majority of protein digestion products actually enter the portal vein in the form of amino acids. Although the basolateral efflux of amino acids occurs via different amino acid transporters, hydrolysis-resistant peptides (and peptide-like drugs) can exit the cell by a basolateral peptide-transporting system that has yet to be identified. The nature of the peptide-transporter(s) at the apical surface of intestinal epithelial cells was revealed once PEPT1 was cloned from a rabbit intestinal cDNA library[22] and shown to be of high capacity and low affinity (Km values in mM range) for di- and tripeptides.[1,4] This transporter has subsequently been cloned in a number of mammalian species including human[23] and mouse.[24] Immunolocalization studies demonstrated that PEPT1 was expressed in the apical membrane of enterocytes in the small intestine (i.e., duodenum, jejunum and ileum) of both species but not in the colon.[5,6] While there is no evidence for PEPT2 in mammalian intestinal epithelia, this protein has been reported in neuromuscular layers of the gastrointestinal tract, and in enteric glial cells and tissue-resident macrophages.[7] PHT1 and PHT2 transcripts have been reported in both human and rat intestinal tissue segments.[8] Moreover, immunohistochemical analyses have indicated that PHT1 is expressed

in the villous epithelium of small intestine,[25] although its subcellular localization remains to be elucidated.

It is generally believed that PEPT1 is the primary (if not sole) transport protein responsible for handling the tremendous variety of di/tripeptides encountered in a physiological setting and the many peptide-like drugs absorbed in a pharmacological setting. However, some experimental findings in intact tissue preparations have suggested that more than one type of peptide carrier may exist.[26] It is also possible that peptide-like drugs are absorbed by multiple transporters. For example, using a rat intestinal perfusion technique, it was suggested that, in addition to the proton-coupled oligopeptide transporter (presumably PEPT1), organic anion and organic cation transporters were involved in the small intestinal uptake of valacyclovir.[27] Regardless, it is clear that the role and relative importance of PEPT1 in the intestine (and other tissues) will not be elucidated by *in vitro*, nonphysiologic studies that lack blood flow as well as appropriate residence times at the critical sites of transport.

The *in vivo* role of PEPT1 in protein nutrition was initially investigated using a deletion mutant of *Caenorhabditis* elegans.[28] In doing so, it was found that abolition of the *Pept1* ortholog in *C.* elegans (i.e., PEP-2) resulted in a severely retarded development as well as reduced progeny and body size. These findings clearly identify intestinal peptide absorption as a key process in body protein homeostasis and contend that rodent models lacking the *Pept1* gene are sorely needed to determine whether or not these findings from the nematode are reproducible in higher organisms.

In the present study, a *Pept1*-deficient mouse model was successfully generated by targeted gene disruption in embryonic stem cells. The PCR analyses confirmed that this mutant mouse strain did not produce the gene to encode *Pept1*. Moreover, the immunoblots demonstrated convincingly that PEPT1 protein was absent from the intestine and kidney of *Pept1*-null mice, while being retained in the same tissues of wild-type mice. As expected, the high-affinity peptide transporter PEPT2 was absent from the intestine but retained in the kidney of *Pept1*-deficient animals. With the loss of PEPT1 in the intestine, the jejunal uptake and permeability of GlySar was drastically reduced during the *in vitro* and *in situ* studies, respectively, when comparing wild-type and *Pept1*-null mice. These studies were subsequently confirmed by *in vivo* experiments in which the oral absorption of GlySar in *Pept1*-deficient animals was one-half that of *Pept1*-competent animals. In contrast, *Pept1* deletion had no effect on the systemic exposure of GlySar following intravenous administration.

Because of the lack of apparent biological effects, it is possible that other POT family members may be upregulated as a compensatory response to *Pept1* gene deletion. However, immunoblot analyses revealed that PEPT2 protein was not aberrantly expressed in the small intestine of *Pept1* null mice, and that the change of PEPT2 expression in kidney was unremarkable. Moreover, the real-time PCR studies demonstrated that PHT1 and PHT2 mRNA were not significantly different in the small intestine, colon and kidney of wild-type and *Pept1* null animals. Thus, an adaptive response by related peptide transporters is very unlikely to explain the lack of a prominent phenotype in *Pept1* null mice. Alternatively, if the brush border membrane enzymes (e.g., peptidases) were upregulated along with amino acid transporters (to handle the increased load), then PEPT1 would not be necessary for the maintenance of protein nutrition. Notwithstanding this uncertainty, our studies have demonstrated definitely that a transport defect of dipeptide absorption occurs in the small intestine. By challenging our transgenic mice in subsequent studies, it is possible that unique, pathological phenotypes will be revealed. This scenario was certainly exemplified when *Mdr1(-/-)* mice died suddenly after a chance encounter with the anthelmintic pesticide ivermectin,[29] when *Bcrp1(-/-)* mice developed phototoxic ear lesions when being fed a diet containing alfalfa,[30] and when *Pept2 (-/-)* mice developed neurotoxicity during chronic dosing of 5-aminolevulinic acid.[31]

The quantitative relevance of PEPT1 between genotypes is quite dramatic when comparing the everted ring uptakes and single-pass perfusions of GlySar in jejunal tissue. Based on the *in vitro* intestinal uptake studies, PEPT1 accounts for about 80% of the total uptake process. Likewise, results form the *in situ* perfusion studies suggest that PEPT1 accounts for about 95% of the total uptake process. The *in vivo* findings, although to a lesser extent, corroborate the *in vitro* and *in situ* results, and support a major role for PEPT1 in the intestinal absorption of GlySar (and presumably other di- and tripeptides). Paracellular transport was not different between wild-type and *Pept1* null mice, as suggested by perfusion studies with mannitol (data not shown), thereby excluding this mechanism as a possible factor in explaining any differences in uptake between the genotypes.

In addition to its role in the intestinal absorption and renal reabsorption of peptide-bound amino acids generated from the diet, PEPT1 has significance in the pharmacology and pharmacokinetics of several therapeutic agents, and as a target for drug delivery strategies.[32] Moreover, PEPT1 has recently been implicated in inflammatory bowel disease, as a potential target in the development of anti-inflammatory therapies, and as a gateway to the innate immune response.[9] It is our view that *Pept1* null mice will offer scientists and clinicians an unparalleled opportunity to examine the role, relevance, and regulation of this peptide transporter under a variety of physiologic, pharmacologic and pathophysiologic conditions.

Acknowledgments

This work was supported in part by grant R01 GM035498 (to DES), Deltagen and Lilly Research Laboratories.

References

(1). Daniel H, Kottra G. The proton oligopeptide cotransporter family SLC15 in physiology and pharmacology. Pflugers Arch 2004;447:610–618. [PubMed: 12905028]

(2). Herrera-Ruiz D, Knipp GT. Current perspectives on established and putative mammalian oligopeptide transporters. J. Pharm. Sci 2003;92:691–714. [PubMed: 12661057]

(3). Rubio-Aliaga I, Daniel H. Mammalian peptide transporters as targets for drug delivery. Trends Pharmacol. Sci 2002;23:434–440. [PubMed: 12237156]

(4). Daniel H, Rubio-Aliaga I. An update on renal peptide transporters. Am. J. Physiol 2003;284:F885–F892.

(5). Walker D, Thwaites DT, Simmons NL, Gilbert HJ, Hirst BH. Substrate upregulation of the human small intestinal peptide transporter, hPepT1. J. Physiol 1998;507:697–706. [PubMed: 9508831]

(6). Groneberg DA, Döring F, Eynott PR, Fischer A, Daniel H. Intestinal peptide transport: Ex vivo uptake studies and localization of peptide carrier PEPT1. Am. J. Physiol. Gastrointest. Liver Physiol 2001;281:G697–G704. [PubMed: 11518682]

(7). Rühl A, Hoppe S, Frey I, Daniel H, Schemann M. Functional expression of the peptide transporter PEPT2 in the mammalian enteric nervous system. J. Comp. Neurol 2005;490:1–11. [PubMed: 16041713]

(8). Herrera-Ruiz D, Wang Q, Gudmundsson OS, Cook TJ, Smith RL, Faria TN, Knipp GT. Spatial expression patterns of peptide transporters in the human and rat gastrointestinal tracts, Caco-2 in vitro cell culture model, and multiple human tissues. AAPS PharmSci 2001;3(1):E9. [PubMed: 11741260]PMID: 11741260

(9). Charrier L, Merlin D. The oligopeptide transporter hPepT1: Gateway to the innate immune response. Lab. Invest 2006;86:538–546. [PubMed: 16652110]

(10). Dalmasso G, Charrier-Hisamuddin L, Nguyen HTT, Yan Y, Sitaraman S, Merlin D. PepT1-mediated tripeptide KPV uptake reduces intestinal inflammation. Gastroenterology 2008;134:166–178. [PubMed: 18061177]

(11). Ruby NF, Brennan TJ, Xie X, Cao V, Franken P, Heller HC, O'Hara BF. Role of melanopsin in circadian responses to light. Science 2002;298:2211–2213. [PubMed: 12481140]

(12). Akarawut W, Lin C-J, Smith DE. Noncompetitive inhibition of glycylsarcosine transport by quinapril in rabbit renal brush border membrane vesicles: Effect on high-affinity peptide transporter. J. Pharmacol. Exp. Ther 1998;287:684–690. [PubMed: 9808697]

(13). Ganapathy V, Mendicino JF, Leibach FH. Transport of glycyl-L-proline into intestinal and renal brush border vesicles from rabbit. J. Biol. Chem 1981;256:118–124. [PubMed: 7451429]

(14). Shen H, Smith DE, Yang T, Huang YG, Schnermann JB, Brosius FC 3rd. Localization of PEPT1 and PEPT2 proton-coupled oligopeptide transporter mRNA and protein in rat kidney. Am. J. Physiol 1999;276:F658–F665. [PubMed: 10330047]

(15). Shen H, Smith DE, Keep RF, Brosius FC 3rd. Immunolocalization of the proton-coupled oligopeptide transporter PEPT2 in developing rat brain. Mol. Pharm 2004;1:248–256. [PubMed: 15981584]

(16). Stewart BH, Chan OH, Jezyk N, Fleisher D. Discrimination between drug candidates using models for evaluation of intestinal absorption. Adv. Drug Deliv. Rev 1997;23:27–45.

(17). Adachi Y, Suzuki H, Sugiyama Y. Quantitative evaluation of the function of small intestinal P-glycoprotein: Comparative studies between in situ and in vitro. Pharm. Res 2003;20:1163–1169. [PubMed: 12948013]

(18). Komiya I, Park JY, Kamani A, Ho NFH, Higuchi WI. Quantitative mechanistic studies in simultaneous fluid flow and intestinal absorption using steroids as model solutes. Int. J. Pharm 1980;4:249–262.

(19). Kou JH, Fleisher D, Amidon GL. Calculation of the aqueous diffusion layer resistance for absorption in a tube: Application to intestinal membrane permeability determination. Pharm. Res 1991;8:298–305. [PubMed: 2052515]

(20). Gibaldi, M.; Perrier, D. Pharmacokinetics. Vol. 2nd ed.. Marcel Dekker Inc.; New York: 1982. p. 409-417.

(21). Ganapathy, V.; Gupta, N.; Martindale, RG. Protein digestion and absorption. In: Johnson, LR., editor. Physiology of the Gastrointestinal Tract. Vol. 4th ed.. Elsevier; Burlington: 2006. p. 1667-1692.

(22). Fei Y-J, Kanai Y, Nussberger S, Ganapathy V, Leibach FH, Romero MF, Singh SK, Boron WF, Hediger MA. Expression cloning of a mammalian proton-coupled oligopeptide transporter. Nature 1994;368:563–566. [PubMed: 8139693]

(23). Liang R, Fei Y-J, Prasad PD, Ramamoorthy S, Han H, Yang-Feng TL, Hediger MA, Ganapathy V, Leibach FH. Human intestinal H^+/peptide cotransporter: Cloning, functional expression, and chromosomal localization. J. Biol. Chem 1995;270:6456–6463. [PubMed: 7896779]

(24). Fei Y-J, Sugawara M, Liu JC, Li HW, Ganapathy V, Ganapathy ME, Leibach FH. cDNA structure, genomic organization, and promoter analysis of the mouse intestinal peptide transporter PEPT1. Biochim Biophys Acta 2000;1492:145–154. [PubMed: 11004485]

(25). Bhardwaj RK, Herrera-Ruiz D, Eltoukhy N, Saad M, Knipp GT. The functional evaluation of human peptide/histidine transporter 1 (hPHT1) in transiently transfected COS-7 cells. Eur. J. Pharm. Sci 2006;27:533–542. [PubMed: 16289537]

(26). Daniel H. Molecular and integrative physiology of intestinal peptide transport. Ann Rev Physiol 2004;66:361–384. [PubMed: 14977407]

(27). Sinko PJ, Balimane PV. Carrier-mediated intestinal absorption of valacyclovir, the L-valyl ester prodrug of acyclovir: 1. Interactions with peptides, organic anions and organic cations in rats. Biopharm Drug Dispos 1998;19:209–217. [PubMed: 9604120]

(28). Meissner B, Boll M, Daniel H, Baumeister R. Deletion of the intestinal peptide transporter affects insulin and TOR signaling in Caenorhabditis elegans. J. Biol. Chem 2004;279:36739–36745. [PubMed: 15155758]

(29). Schinkel AH, Smit JJM, van Tellingen O, Beijnen JH, Wagenaar E, van Deemter L, Mol CAAM, van der Valk MA, Robanus-Maandag EC, te Riele HPJ, Berns AJM, Borst P. Disruption of the mouse mdr1a p-glycoprotein gene leads to a deficiency in the blood-brain barrier and to increased sensitivity to drugs. Cell 1994;77:491–502. [PubMed: 7910522]

(30). Jonker JW, Buitelaar M, Wagenaar E, van der Valk MA, Scheffer GL, Scheper RJ, Plosch T, Kuipers F, Elferink RF, Rosing H, Beijnen JH, Schinkel AH. The breast cancer resistance protein protects

against a major chlorophyll-derived dietary phototoxin and protoporphyria. Proc. Natl. Acad. Sci. U. S. A 2002;99:15649–15654. [PubMed: 12429862]

(31). Hu Y, Shen H, Keep RF, Smith DE. Peptide transporter 2 (PEPT2) expression in brain protects against 5-aminolevulinic acid neurotoxicity. J. Neurochem 2007;103:2058–2065. [PubMed: 17854384]

(32). Brandsch M, Knütter I, Bosse-Doenecke E. Pharmaceutical and pharmacological importance of peptide transporters. J. Pharm. Pharmacol 2008;60:543–585. [PubMed: 18416933]

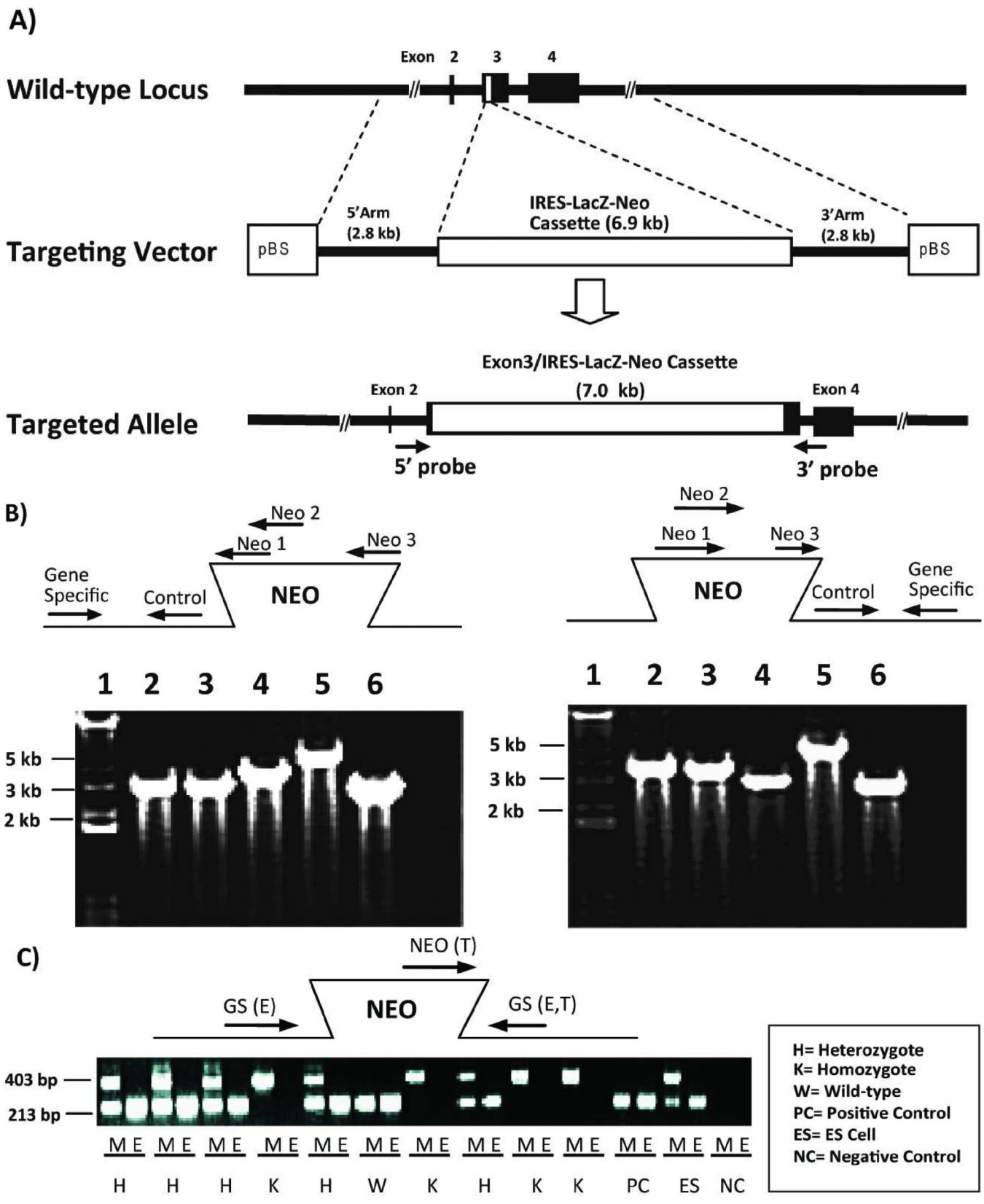

Figure 1.

Schematic of the genomic *Pept1* locus, targeting vector and mutated allele (A). The endogenous locus is depicted by thick solid lines or filled boxes. The small open box within exon 3 of the wild-type locus (top) represents a 25 bp region that was replaced with a 6.9 kb IRES-LacZ-Neo cassette. The IRES-LacZ-Neo locus is depicted in the open box (middle), and the 5' and 3' probes utilized for PCR of the homologous recombinants are represented by solid arrows (bottom). Genomic DNA from the recombinant ES cell line was assayed for homologous recombination by PCR in both the 5' and 3' directions (B). The figure represents the design and results of three separate primers in the neomycin insert paired with gene-specific primers. Lane 1 is a 1.0 kB ladder; lanes 2, 3 and 4 are the PCR product using neo 1, 2 and 3 primers, respectively, paired with gene-specific primers; lane 5 is a DNA sample control and lane 6 is the positive control. Genotyping results via PCR from mouse tail biopsies (C). The schematic demonstrates the PCR primer strategy to detect the endogenous (213 bp) or targeted (403 bp) allele. The reaction “M” for each sample includes the neomycin primer (NEO) and gene-specific primers (GS), and detects the endogenous (E) and targeted (T) alleles. The reaction “E” contains only the GS primers and detects only the endogenous allele.

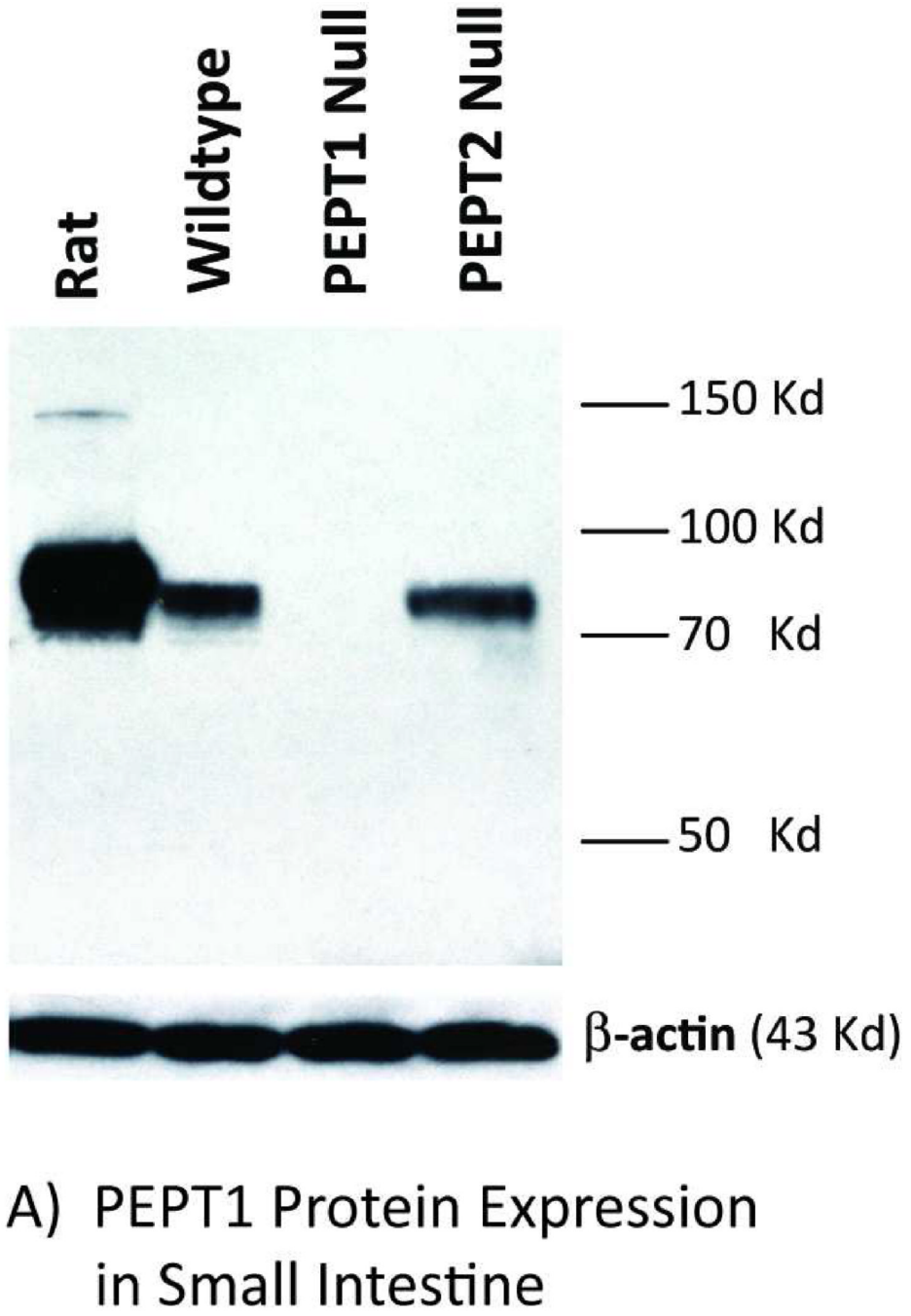

Figure 2.
PEPT1 protein expression in brush border membrane vesicles of small intestine (A) and kidney (B). Apical membranes were pooled from six 8-week old mice or a single adult rat and subjected to 7.5% SDS-PAGE (50 μg of protein for intestine of both species; 40 μg of protein for rat kidney and 100 μg of protein for mouse kidney).

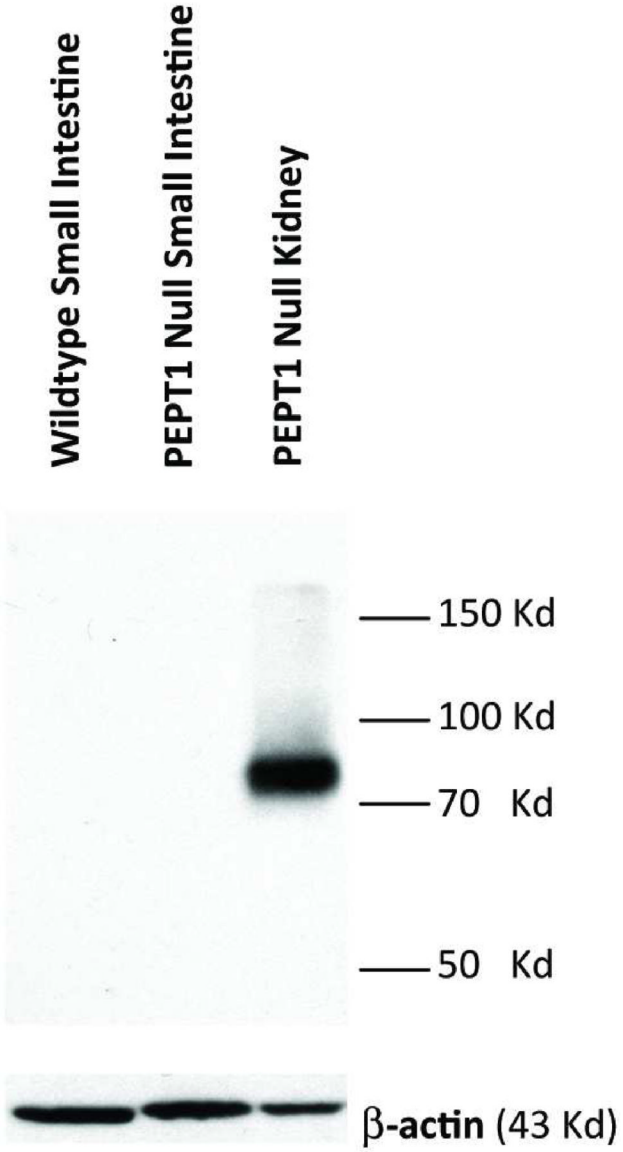

A) PEPT2 Protein Expression in Small Intestine and Kidney

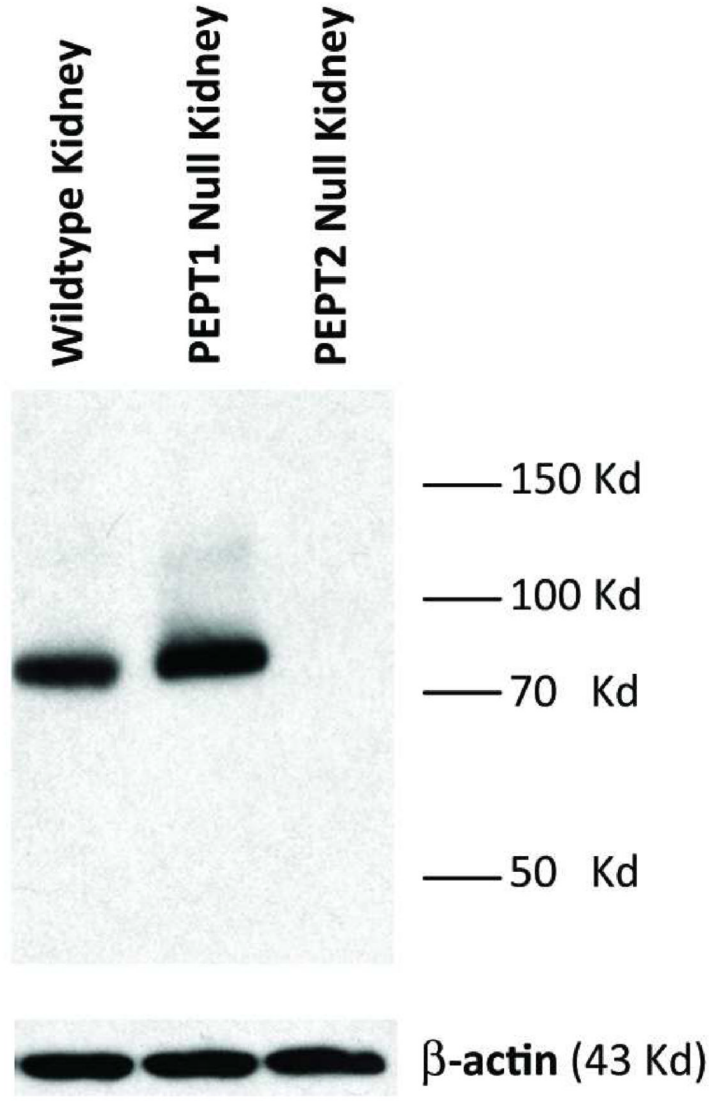

B) PEPT2 Protein Expression in Kidney Vesicles

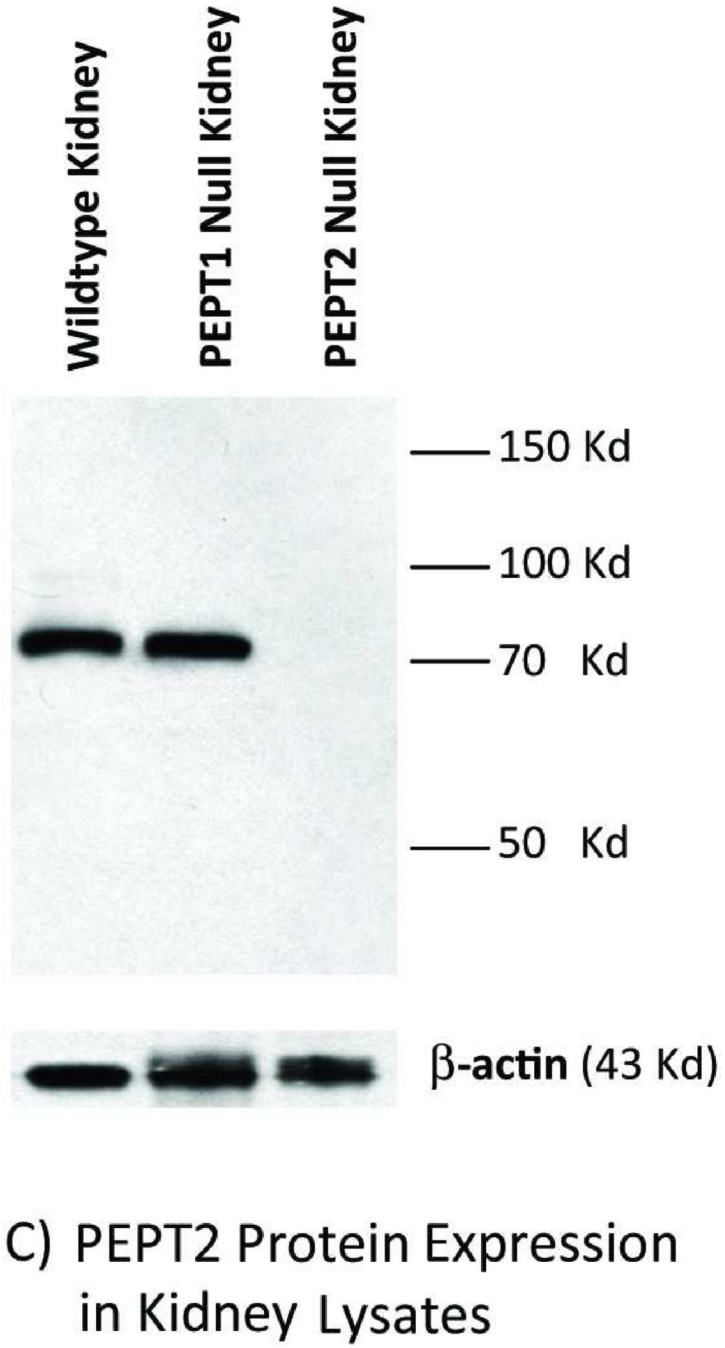

Figure 3.

PEPT2 protein expression in brush border membrane vesicles of mouse small intestine (A) and kidney (A or B), and whole tissue lysates of mouse kidney (C). Apical membranes and lysates were pooled from six 8-week old mice and subjected to 7.5% SDS-PAGE (20 μg of protein for mouse intestine and kidney vesicles; 90 μg of protein for mouse kidney lysates).

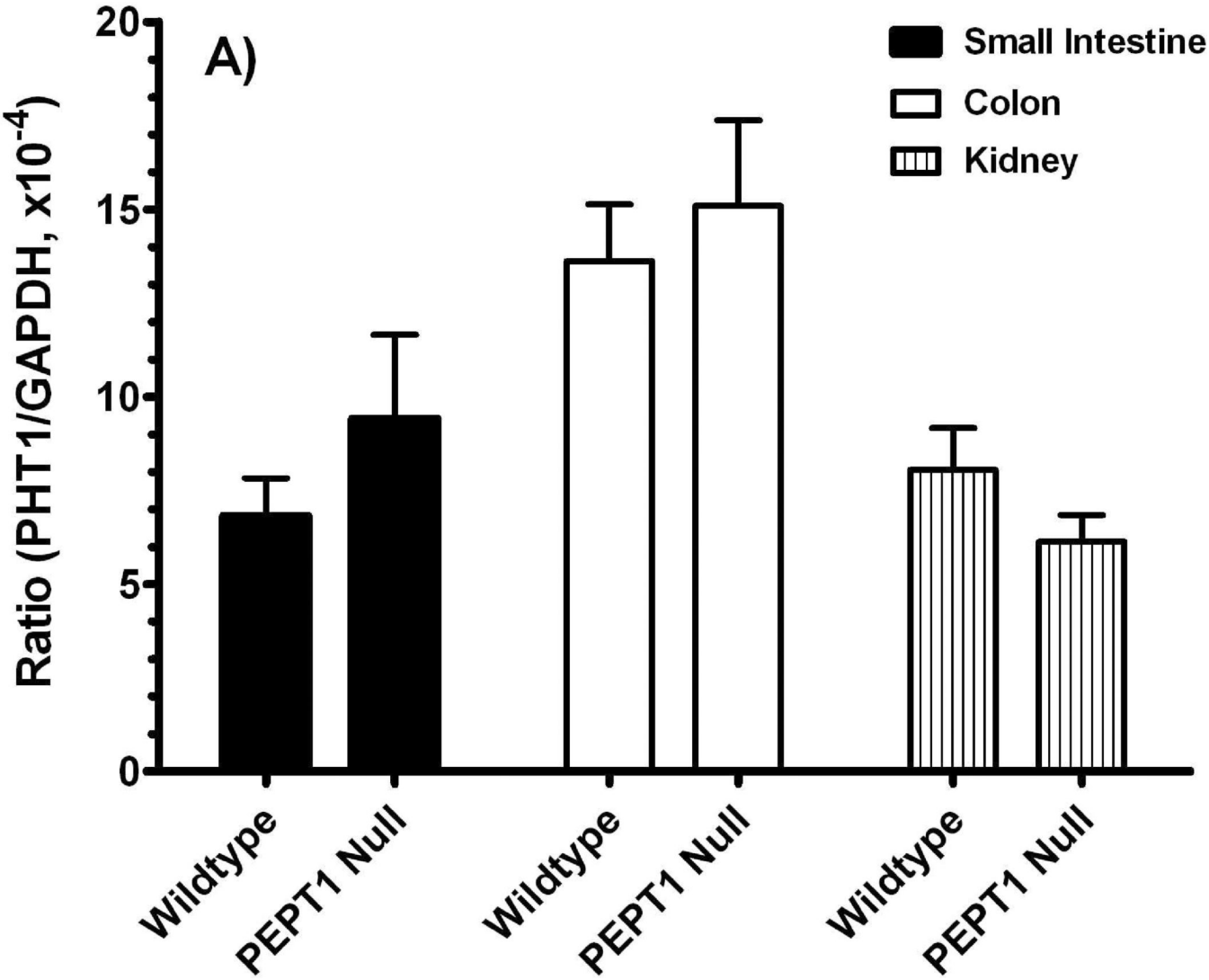

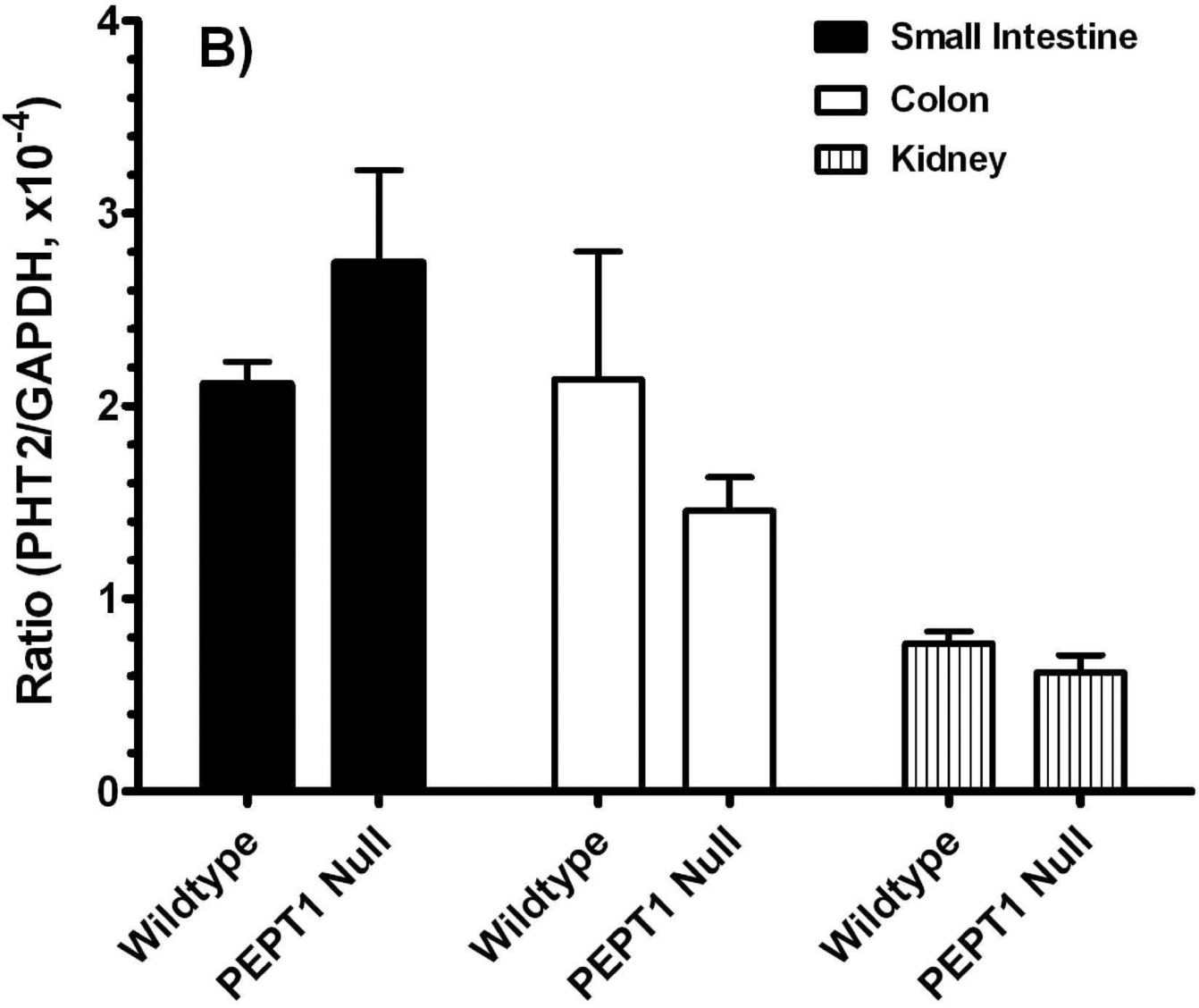

Figure 4.
Real time-PCR analyses for PHT1 (A) and PHT2 (B) transcripts in the small intestine, colon and kidney of wild-type and *Pept1* null mice (n=6, mean±SE).

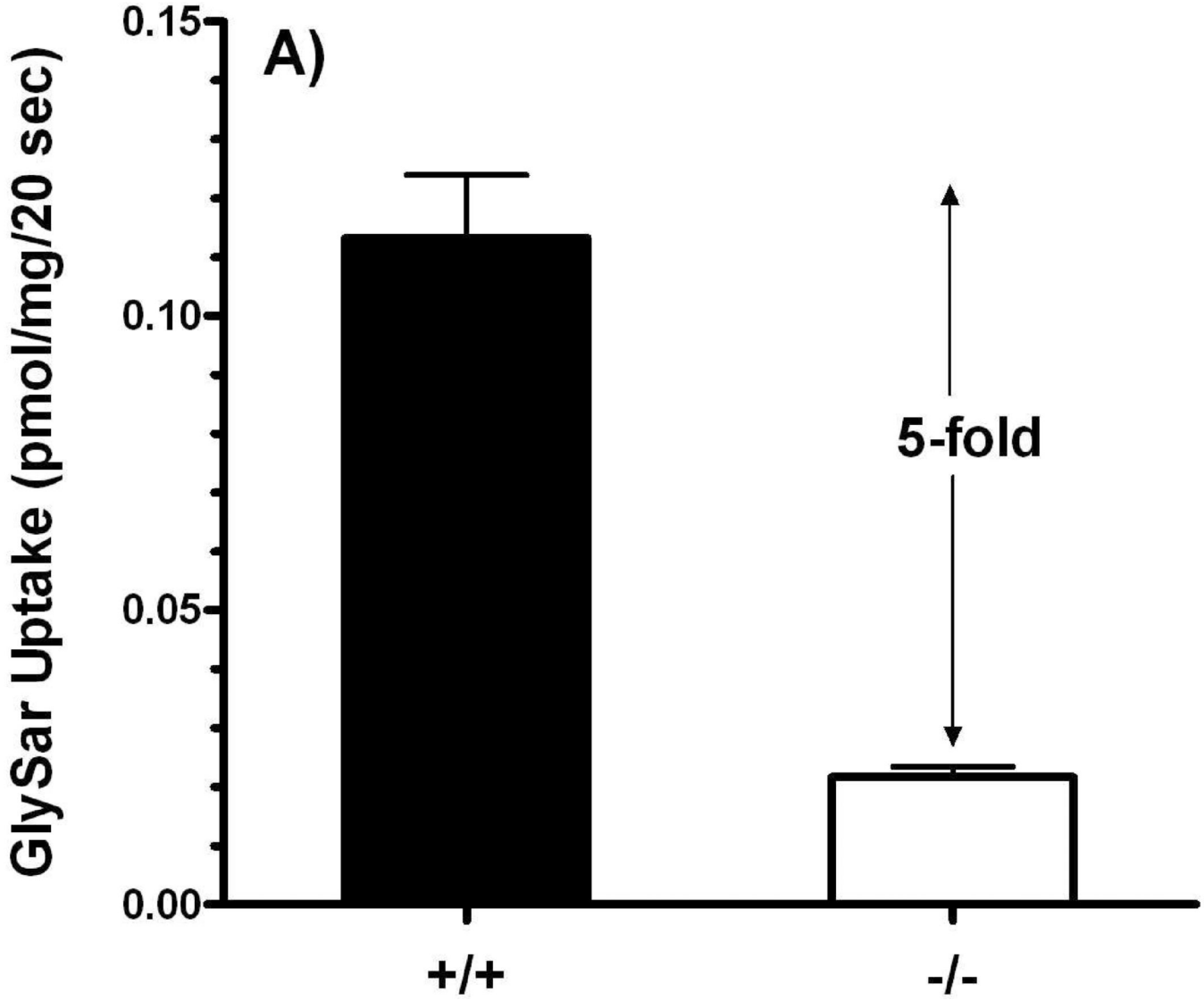

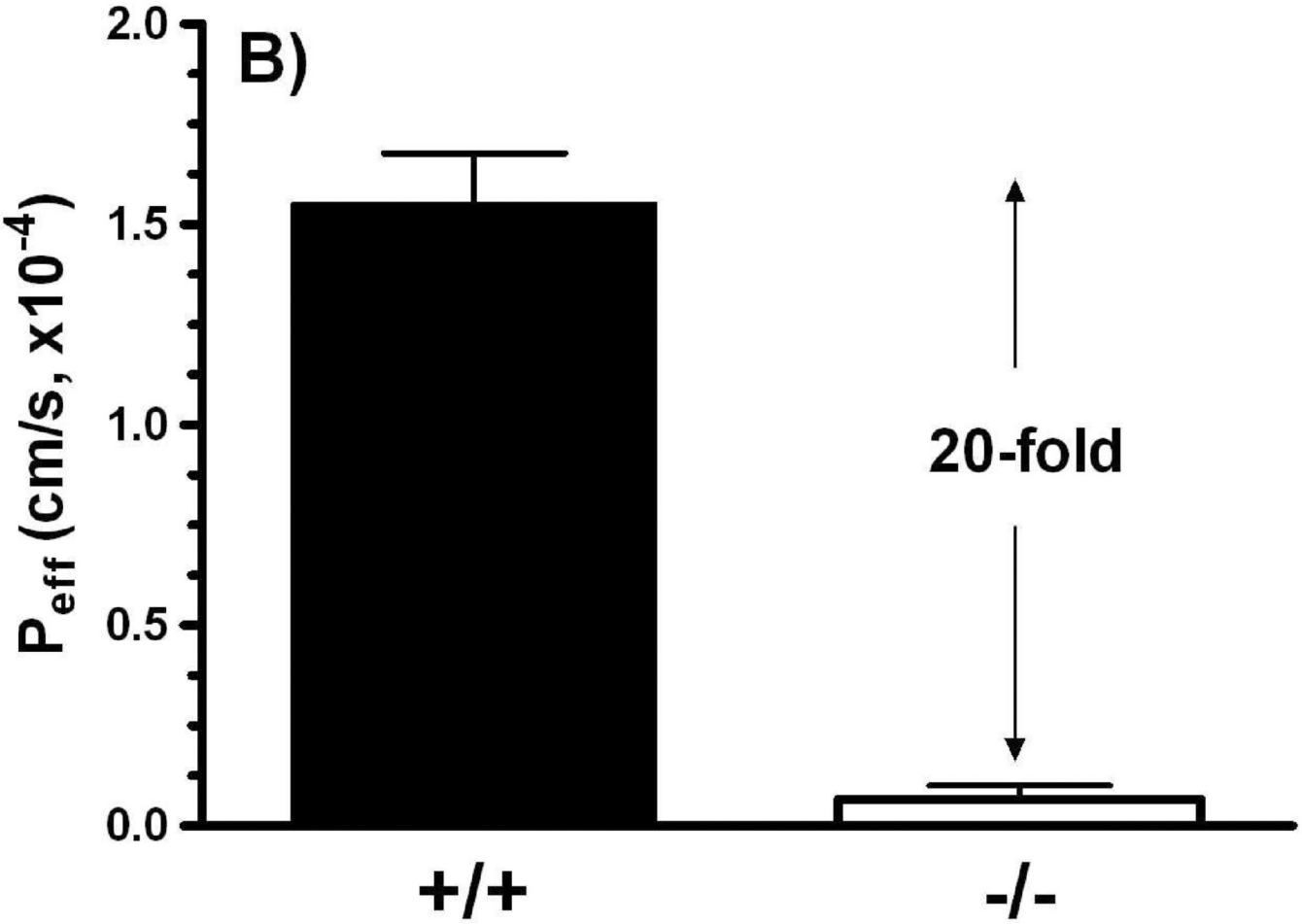

Figure 5.

Intestinal uptake (A) of 4 μM [^{3}H]GlySar into everted jejunal rings of wild-type (+/+) and *Pept1* null (-/-) mice. Studies were performed in pH 6.0 buffer (n=3, mean±SE; $p<0.001$). Effective permeability (B) of 10 μM [^{3}H]GlySar during jejunal perfusions of wild-type and *Pept1* null mice. Studies were performed in pH 6.5 buffer (n=6, mean±SE; $p<0.001$).

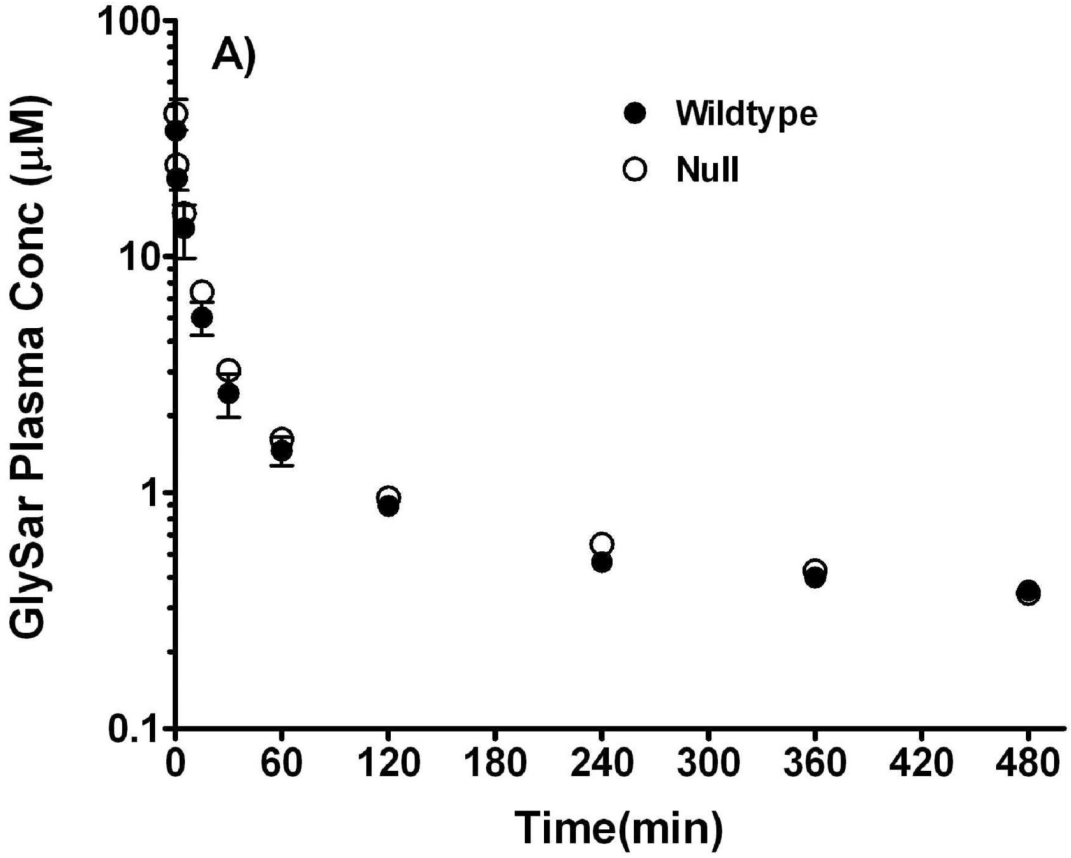

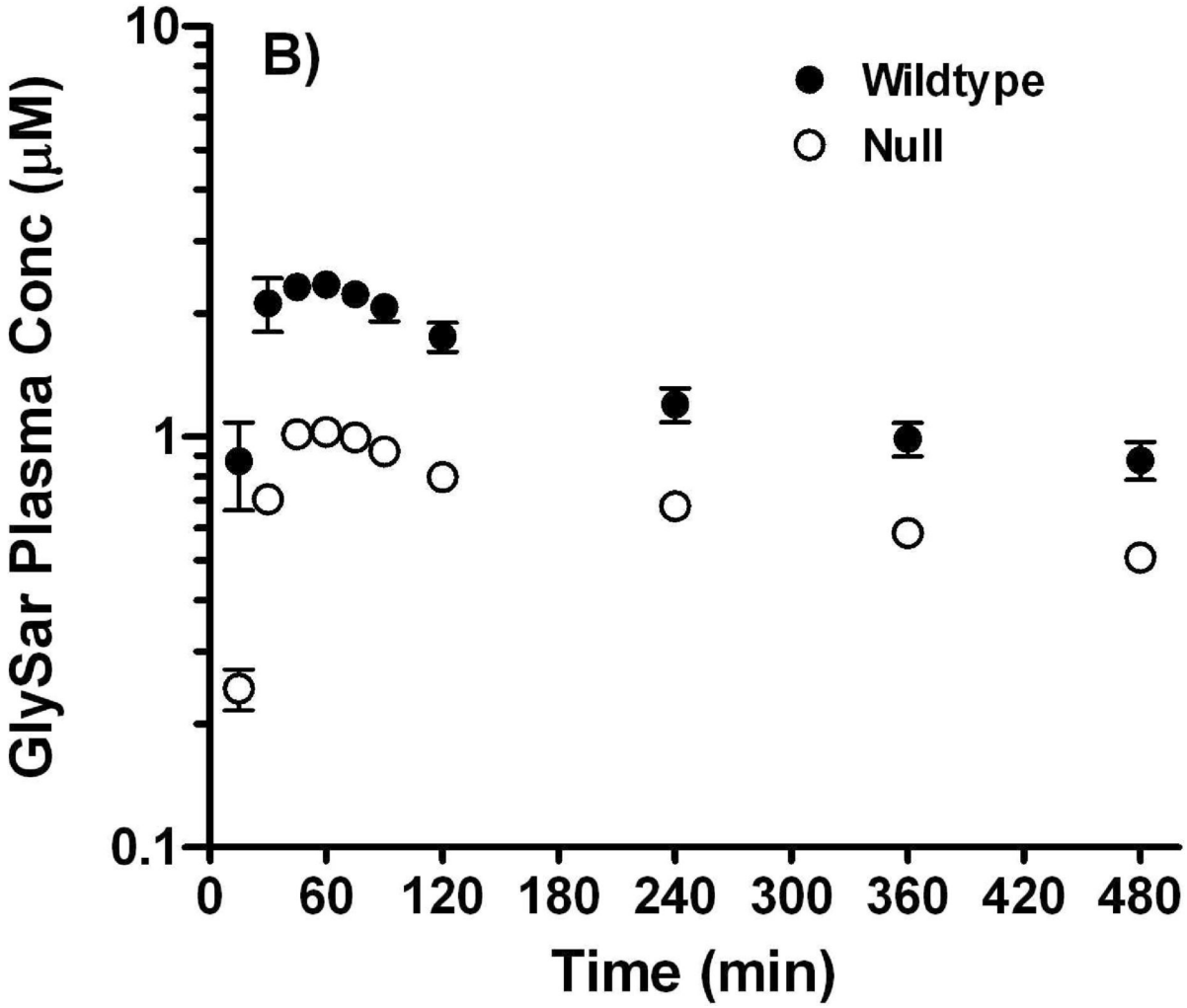

Figure 6.
Plasma concentration vs. time curves of [^{14}C]GlySar after intravenous (A) and gastric gavage (B) doses of dipeptide (5 nmol/g body weight) in wild-type and *Pept1* null mice (n=3-4, mean ±SE).

Table 1

Serum clinical chemistry of *Pept1*$^{-/-}$, *Pept1*$^{+/+}$, and *C57BL6* Mice

Parameter	*Pept1*$^{-/-}$	*Pept1*$^{+/+}$	*C57BL/6*
Body Weight, 7 wk (g)	24.4 ± 1.5	23.4 ± 4.6	24.1 ± 2.7
Serum			
Sodium (mmol/liter)	139 ± 3	141 ± 2	142 ± 1
Potassium (mmol/liter)	5.9 ± 0.7	6.2 ± 0.6	5.0 ± 0.3
Chloride (mmol/liter)	100 ± 2	102 ± 3	103 ± 32
Glucose (mg/dl)	245 ± 56	239 ± 38	264 ± 8
Bicarbonate (mg/dl))	17.7 ± 1.5	17.8 ± 1.1	18.3 ± 1.5
Calcium (mg/dl)	9.9 ± 0.3	10.2 ± 0.3	9.8 ± 0.1
Bilirubin (mg/dl)	0.1 ± 0.0	0.1 ± 0.0	0.1 ± 0.0
Urea Nitrogen (mg/dl)	23.4 ± 4.6	24.1 ± 2.7	23.2 ± 4.1
Alkaline Phosphatase (units/liter)	174 ± 34	175 ± 30	196 ± 25
Alanine Transaminase (units/liter)	33.3 ± 18.9	48.5 ± 10.8	35.0 ± 18.6
Aspartate Aminotransferase (units/liter)	95.9 ± 44.4	139 ± 55	98.8 ± 74.2
Protein (g/dl)	4.9 ± 0.2	5.0 ± 0.1	4.8 ± 0.3
Albumin (g/dl)	1.3 ± 0.1	1.4 ± 0.0	1.4 ± 0.3

Results are mean ± SD (n=4-6 for *Pept1*$^{-/-}$ F2, *Pept1*$^{+/+}$ F2, and *C57BL/6* mice).